

Collision between Chaotic and Periodic Attractors in a Ring of Coupled Chaotic Circuits

Yoko Uwate

Dept. of Electrical and Electronic Engineering,
Tokushima University
2-1 Minami-Josanjima, Tokushima, Japan
Email: uwate@ee.tokushima-u.ac.jp

Yoshifumi Nishio

Dept. of Electrical and Electronic Engineering,
Tokushima University
2-1 Minami-Josanjima, Tokushima, Japan
Email: nishio@ee.tokushima-u.ac.jp

Abstract—In this study, we investigate synchronization phenomena observed in coupled chaotic circuits as a ring topology when two types of the bifurcation parameters to generate chaotic and three-periodic attractors are arranged. By using computer simulations and circuit experiments, we observe a collision between chaotic and periodic attractors depending on the number of chaotic attractors and the location of chaotic attractors in the system.

I. INTRODUCTION

Synchronization and the related bifurcation of chaotic systems are good models to describe various higher-dimensional nonlinear phenomena in the field of natural science. In particular, the breakdown of chaos synchronization has attracted many researchers' attentions and their mechanisms have been gradually made clear [1]-[8]. However, a lot of phenomena around chaos synchronization are still veiled as well as other nonlinear circuits problems. Hence, in order to understand and exploit such phenomena, it is important to discover them, to model them, and to investigate them.

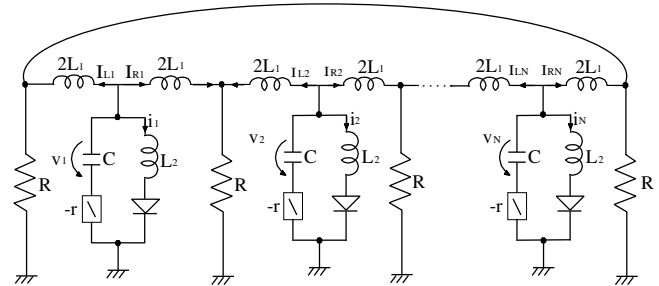
On the other hand, it is important to investigate synchronization phenomena of coupled circuits under a difficult situation for the circuits. For examples, there are some frustrations in the circuit systems such as the coupling structure, frequency errors and external stimuli. Setou et al. have observed interesting synchronization phenomena when van der Pol oscillators with different oscillation frequencies are coupled by a resistor as a star topology [9]. We have investigated a ring consisting of van der Pol oscillators with different oscillation frequencies. By using computer simulations, oscillation death, independent oscillation and double-mode oscillation were observed [10][11]. We consider that if coupled circuits with more different characteristics are coupled, the coupled circuits feel the frustrations more strongly.

In this study, we investigate synchronization phenomena observed in coupled chaotic circuits as a ring topology when the chaotic circuits generating chaotic and three-periodic attractors are arranged in the circuit system. By using computer simulations and circuit experiments, we observe a collision between chaotic and periodic attractors when the ratio of chaotic attractor is larger than the periodic attractor. After the collision, the periodic attractor arranged in the next to the chaotic attractor produce the bursting part such as intermittency-like

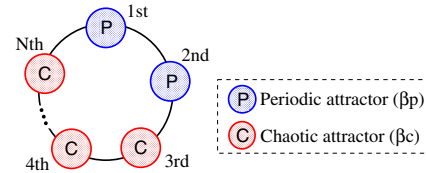
chaos. And, chaos degree of the chaotic attractor becomes weak by the effects of the adjacent periodic attractor.

II. CIRCUIT MODEL

In this study, we consider a ring of the chaotic circuits as shown in Fig. 1. In the circuit system, two adjacent chaotic circuits are coupled by a resistor R via an inductor of each chaotic circuit. By using this coupling method, two adjacent circuits tend to synchronize with anti-phase state.



(a) Ring of coupled chaotic circuits.



(b) Conceptual circuit model.

Fig. 1. Coupled chaotic circuits as a ring topology.

First, the $i-v$ characteristics of the diodes are approximated by two-segment piecewise-linear functions as

$$v_d(i_k) = \frac{1}{2}(r_d i_k + E - |r_d i_k - E|). \quad (1)$$

By changing the variables and parameters,

$$\begin{aligned} I_{Rk} &= \sqrt{\frac{C}{L_1}} E x_{Rk}, & I_{Lk} &= \sqrt{\frac{C}{L_1}} E x_{Lk}, \\ i_k &= \sqrt{\frac{C}{L_1}} E y_k, & v_k &= E z_k, & t &= \sqrt{L_1 C} \tau, \\ \alpha &= \frac{L_1}{L_2}, & \beta &= r \sqrt{\frac{C}{L_1}}, & \gamma &= R \sqrt{\frac{C}{L_1}}, & \delta &= r_d \sqrt{\frac{C}{L_1}}, \end{aligned} \quad (2)$$

the normalized circuit equations are given as

$$\left\{ \begin{array}{l} \frac{dx_{Rk}}{d\tau} = \frac{1}{2} \{ \beta(x_{Rk} + x_{Lk} + y_k) - z_k \\ \quad - \gamma(x_{Rk} + x_{L(k+1)}) \} \\ \frac{dx_{Lk}}{d\tau} = \frac{1}{2} \{ \beta(x_{Rk} + x_{Lk} + y_k) - z_k \\ \quad - \gamma(x_{Lk} + x_{R(k-1)}) \} \\ \frac{dy_k}{d\tau} = \alpha \{ \beta(x_{Rk} + x_{Lk} + y_k) - z_k - f(y_k) \} \\ \frac{dz_k}{d\tau} = x_{Rk} + x_{Lk} + y_k \end{array} \right. \quad (k = 1, 2, \dots, N) \quad (3)$$

where

$$x_{L0} = 0, \quad x_{R(N+1)} = 0, \quad (4)$$

$$f(y_k) = 0.5 (\delta y_k + 1 - |\delta y_k - 1|). \quad (5)$$

In these equations, γ is the coupling strength, N is the number of coupled chaotic circuits and β denotes the bifurcation parameter. By changing β , the obtained attractors are controlled. We define β_c to generate the chaotic attractors, and β_p is defined to generate the three-periodic attractors.

For the computer simulations, we calculate Eq. (3) using the fourth-order Runge-Kutta method with step size $h = 0.005$. We set the parameters of this circuit model as follows; $\alpha = 7.0$, $\beta_c = 0.175$, $\beta_p = 0.160$ and $\gamma = 0.01$.

III. SYNCHRONIZATION PHENOMENA

A. $N=3$

Table I summarizes the observed phenomena for coupling oscillator number $N = 3$ by changing the bifurcation parameter β_c . In these tables, “P” denotes *three-periodic attractor*, “(P)” denotes *three-periodic attractor with oscillation*, “C” denotes *chaotic attractor*, “I” is *intermittency-like chaos* and $T = 1e + 05[\tau]$. The initial circuit arrangement of the chaotic and the three-periodic attractors is shown in the middle row in the tables. From these tables, we can see that the collisions are occurred between the chaotic and the three-periodic attractors. Namely, the three-periodic attractors are attracted by the bursting behavior form the adjacent chaotic circuits and three-periodic attractors behaves like the intermittency-like chaos near the three-periodic window.

TABLE I
ATTRACTOR (N=3)

β_c	Initial State ($\tau = 0$)			Steady State ($\tau = T$)		
	1st	2nd	3rd	1st	2nd	3rd
$\beta_c = 0.165$	P	P	C	(P)	(P)	C
	P	C	C	(P)	C	C
$\beta_c = 0.175$	P	P	C	(P)	(P)	C
	P	C	C	I	C	C
$\beta_c = 0.185$	P	P	C	I	I	C
	P	C	C	I	C	C

Next, the phase difference between the adjacent circuits are summarized in Table. II. “Non-syn” in these tables means the asynchronization. The same attractors are synchronized at

anti-phase state. However, the chaotic and the three-periodic attractors could not be synchronized.

TABLE II
PHASE DIFFERENCE (N=3)

	Period-Period	Period-Chaos	Chaos-Chaos
Phase	Anti-phase	Non-syn.	Anti-phase

As one example, the observed attractors and the phase differences by using the computer simulations (initial pattern: (P-C-C) in Table I) are shown in Fig. 2. We also confirm the similar attractors and the phase differences in circuit experiments as shown in Fig. 3.

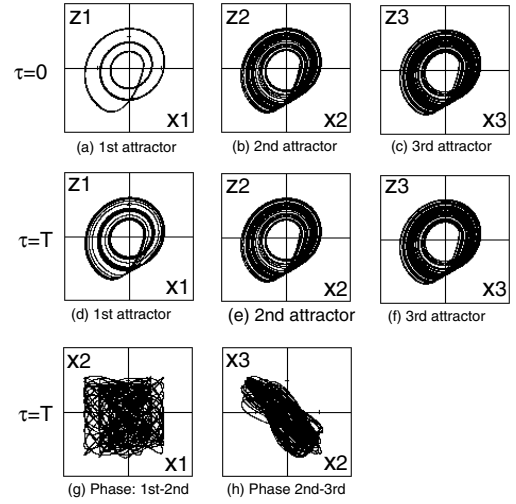


Fig. 2. Attractors and phase difference (computer simulations), $\alpha = 7.0$, $\beta_p = 0.160$, $\beta_c = 0.175$, $\delta = 50.0$ and $\gamma = 0.01$.

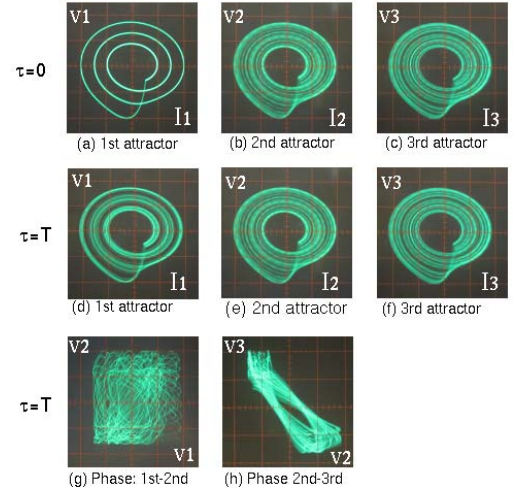


Fig. 3. Attractors and phase difference (circuit experimental results). $L_1 = 300\text{mH}$, $L_2 = 10\text{mH}$, $r_p = 740\Omega$, $r_c = 730\Omega$ and $C = 33\text{nF}$. x-axis:[1V/div], y-axis:[1V/div].

Figure 4 shows the time series of $x_{R1} + x_{L1}$ when the solution of the first circuit across to the Poincaré section ($x_{R1} + x_{L1} < 0$, $z_1 = 0$). We can see that the three-periodic

TABLE III
ATTRACTOR (N=10)

Patt.	Initial State ($\tau = 0$)										Steady State ($\tau = T$)									
	1st	2nd	3rd	4th	5th	6th	7th	8th	9th	10th	1st	2nd	3rd	4th	5th	6th	7th	8th	9th	10th
$\beta_c = 0.175$	P	P	P	P	P	C	P	P	P	P	P	P	P	P	(P)	C	(P)	P	P	P
	P	P	P	P	C	C	P	P	P	P	P	P	P	(P)	C	C	(P)	P	P	P
	P	P	P	P	C	C	C	P	P	P	P	P	P	(P)	C	C	C	(P)	P	P
	P	P	P	C	C	C	C	C	P	P	(P)	I	C	C	C	C	C	C	P	P
	P	P	C	C	C	C	C	C	P	P	(P)	I	C	C	C	C	C	C	(P)	P
	P	C	C	C	C	C	C	C	C	P	(P)	C	C	C	C	C	C	C	C	(P)
	P	C	C	C	C	C	C	C	C	C	I	C	C	C	C	C	C	C	C	C
	P	C	C	C	C	C	C	C	C	C	I	C	C	C	C	C	C	C	C	C
$\beta_c = 0.185$	P	P	P	P	P	C	P	P	P	P	P	P	P	P	(P)	C	(P)	P	P	P
	P	P	P	P	C	C	P	P	P	P	P	P	P	I	C	C	(P)	P	P	P
	P	P	P	P	C	C	C	P	P	P	P	(P)	I	I	C	C	C	I	P	P
	P	P	P	C	C	C	C	P	P	P	P	(P)	C	C	C	C	C	(P)	P	P
	P	P	C	C	C	C	C	C	P	P	(P)	(P)	(P)	4I	4I	4I	4I	4I	(P)	P
	P	P	C	C	C	C	C	C	P	P	P	(P)	(P)	4I	4I	4I	4I	4I	4I	(P)
	P	C	C	C	C	C	C	C	C	P	(P)	4I	4I	4I	4I	4I	4I	4I	4I	I
	P	C	C	C	C	C	C	C	C	C	I	4I	4I	4I	4I	4I	4I	4I	4I	4I

attractor changes to the intermittency-like chaos by influence of adjacent chaotic circuits. We also confirm that the timing of the bursting depends on the circuit parameters such as the bifurcation parameter and coupling strength.

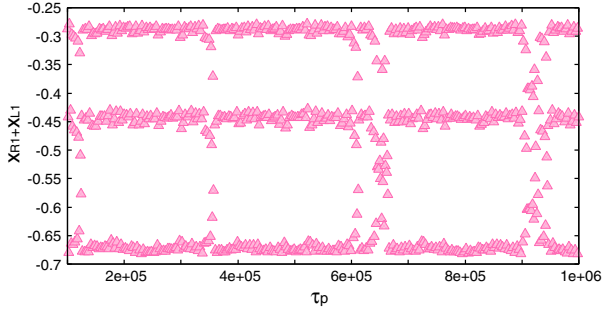


Fig. 4. Intermittency burst (computer simulations). $\alpha = 7.0, \delta = 50.0, \gamma = 0.01, \beta_p = 0.160$ and $\beta_c = 0.175$.

B. N=10

Next, we change the number of coupling circuits to $N = 10$. The computer simulation results are summarized in Table III. The collisions are observed between the chaotic and the periodic attractors. For the case of $\beta_c = 0.175$, the periodic attractors are affected by chaotic factors and are attracted to the intermittency-like chaos or the three-periodic attractor with oscillation. While, in the case of $\beta_c = 0.185$, when the ratio of chaotic attractor is larger than 40%, four-periodic intermittency-like chaos is observed.

Figure 5 shows the two band chaos attractor and four-periodic intermittency-like chaotic attractor observed from the computer simulations. The time wave form of the four-periodic intermittency-like chaos is shown in Fig. 6.

In addition, Fig. 7 shows one examples of synchronization states when the chaotic and the periodic attractors are arranged by irregularly. The horizontal axis is the Poincaré time and the vertical axis shows the value of $x_{Rk} + x_{Lk}$ when the solution of the first circuit crosses to the Poincaré section

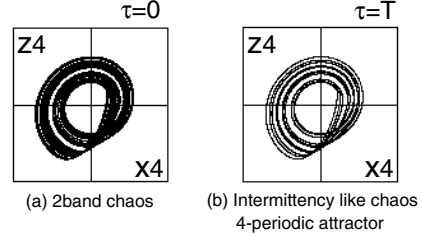


Fig. 5. Intermittency-like chaos four periodic attractor (computer simulations). $\alpha = 7.0, \delta = 50.0, \gamma = 0.01, \beta_p = 0.160$ and $\beta_c = 0.175$.

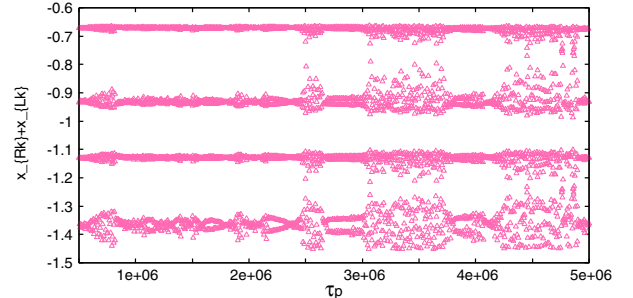


Fig. 6. Intermittency-like chaos four periodic attractor (computer simulations). $\alpha = 7.0, \delta = 50.0, \gamma = 0.01, \beta_p = 0.160$ and $\beta_c = 0.175$.

($x_{R1} + x_{L1} < -1.2, z_1 = 0$). Namely, if the circuit generates chaotic solution the curve of $x_{Rk} + x_{Lk}$ oscillates. While if the circuit generates the periodic solution the curve becomes constant. From these results, when the periodic attractor is located between the chaotic attractors, the periodic attractors are attracted by the bursting behavior from the chaotic circuits and the periodic attractors behaves like the intermittency-like chaos.

IV. APPLICATION FOR LARGE SCALE NETWORKS

Finally, we apply the proposed circuit model to the large-scale networks. Figure 8 shows two examples of synchronization states when the chaotic and the periodic attractors are arranged by irregularly. The horizontal axis is the Poincaré

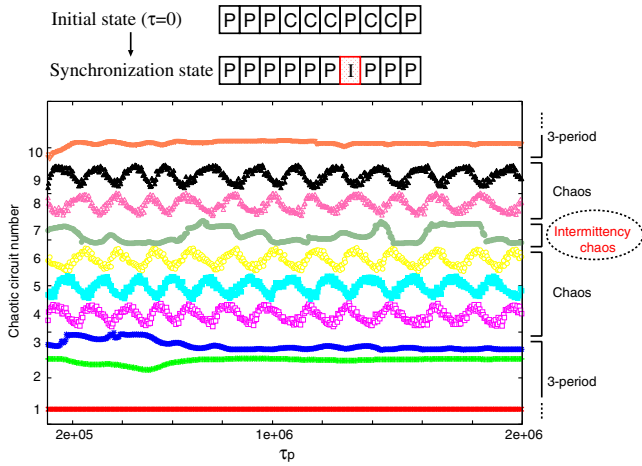


Fig. 7. Synchronization states for $N = 10$ by irregularly arrangement (computer simulations). $\alpha = 7.0, \delta = 50.0, \gamma = 0.01, \beta_p = 0.160$ and $\beta_c = 0.175$.

time and the vertical axis shows the value of $x_{Rk} + x_{Lk}$ when the solution of the first circuit crosses to the Poincaré section ($x_{R1} + x_{L1} < -1.2, z_1 = 0$). In this case, the parameter of the chaotic attractors is fixed with $\beta_c = 0.175$ and $\beta_c = 0.185$. We confirm the complex behavior which is that the periodic attractor changes to the intermittency-like chaos by affecting the chaotic attractor.

The results of the statistical analysis for this large scale network is going to be introduced at the presentation.

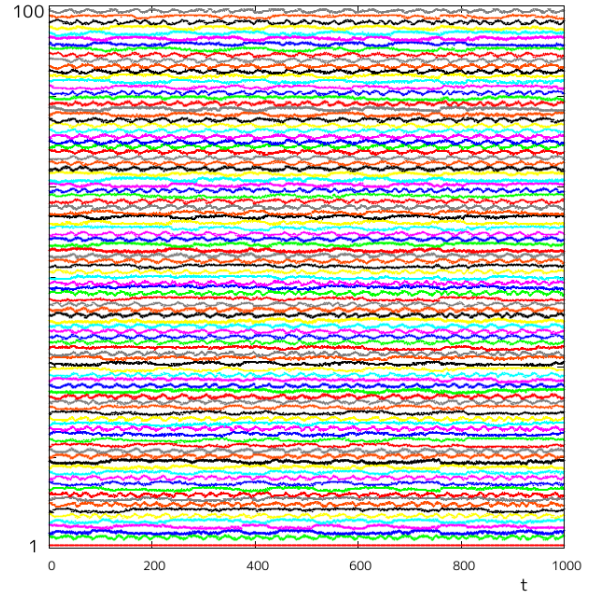
V. CONCLUSION

In this study, we have investigated synchronization phenomena observed in coupled chaotic circuits as a ring topology when two types of the bifurcation parameters to generate chaotic and three-periodic attractors were used. By using computer simulations and circuit experiments, we have observed the clustering phenomena of coupled chaotic circuits depending on the number and the position of the circuits generating chaotic attractors.

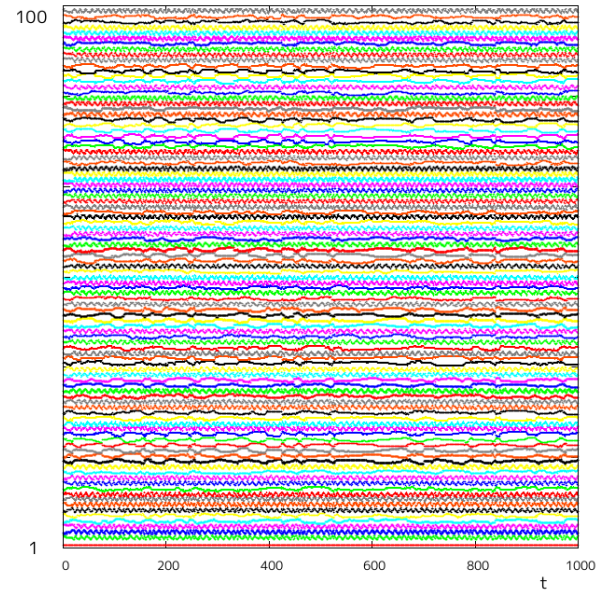
As our future works, we develop an efficient method to analyze the obtained synchronization phenomena of the proposed system. Considering the other types of chaotic circuits and the other coupling methods are also important subjects for us.

REFERENCES

- [1] P. Ashwin, J. Buescu and I. Stewart, *Bubbling of Attractors and Synchronization of Chaotic Oscillators*. Phys. Lett., vol. A193, pp. 126-139, 1994.
- [2] T. Kapitaniak and L.O. Chua, *Locally-Intermingled Basins of Attraction in Coupled Chua's Circuits*. Int. J. Bifurcation and Chaos, vol. 6, no. 2, pp. 357-366, 1996.
- [3] M. Wada, Y. Nishio and A. Ushida, *Analysis of Bifurcation Phenomena on Two Chaotic Circuits Coupled by an Inductor*. IEICE Trans. Fundamentals, vol. E80-A, no. 5, pp. 869-875, May 1997.
- [4] J. Chubb, E. Barreto, P. So and B.J. Gluckman, *The Breakdown of Synchronization in Systems of Nonidentical Chaotic Oscillators: Theory and Experiment*. Int. J. Bifurcation and Chaos, vol. 11, no. 10, pp. 2705-2713, 2001.
- [5] R.L. Viana, C. Grebogi, S.E. de S. Pinto, S.R. Lopes, A.M. Batista and J. Kurths, *Bubbling Bifurcation: Loss of Synchronization and Shadowing Breakdown in Complex Systems*. Physica D, vol. 206, pp. 94-108, 2005.
- [6] C.P. Li, W.H. Deng and D. Xu, *Chaos Synchronization of the Chua System with a Fractional Order*. Physica A, vol. 360, pp. 171-185, 2006.



(a) $\beta_c = 0.175$.



(b) $\beta_c = 0.185$.

Fig. 8. Synchronization state for $N = 100$. $\alpha = 7.0, \delta = 50.0, \gamma = 0.01, \beta_p = 0.160$ and the ratio of chaotic attractor: 50%.

- [7] M. Chen and J. Kurths, *Chaos Synchronization and Parameter Estimation from a Scalar Output Signal*. Phys. Rev. E, vol. 76, 027203, 2007.
- [8] H.T. Yau and J.J. Yan, *Chaos Synchronization of Different Chaotic Systems Subjected to Input Nonlinearity*. Applied Math. and Comp., vol. 197, pp. 775-788, 2008.
- [9] Y. Setou, Y. Nishio and A. Ushida, *Synchronization Phenomena in Resistively Coupled Oscillators with Different Frequencies*. IEICE Trans. Fundamentals, vol. E79-A, no. 10, pp. 1575-1580, 1996.
- [10] Y. Uwate, Y. Nishio and R. Stoop, *Group Synchronization of van der Pol Oscillators with Different Frequencies*. Proc. of NOLTA'08, pp. 612-615, 2008.
- [11] Y. Uwate, Y. Nishio and R. Stoop, *Synchronization of Distant Neighbors Oscillators in a Ring Network*. Proc. of NOLTA'09, pp. 439-442, 2009.